

# Nonlinear Saturation of Stimulated Brillouin Scattering for Long Time Scales

*L. Divol, B.I. Cohen, E.A. Williams, A.B. Langdon, and  
B.F. Lasinski*

This article was submitted to Physical Review Letters

**September 6, 2002**

*U.S. Department of Energy*

Lawrence  
Livermore  
National  
Laboratory

## **DISCLAIMER**

This document was prepared as an account of work sponsored by an agency of the United States Government. Neither the United States Government nor the University of California nor any of their employees, makes any warranty, express or implied, or assumes any legal liability or responsibility for the accuracy, completeness, or usefulness of any information, apparatus, product, or process disclosed, or represents that its use would not infringe privately owned rights. Reference herein to any specific commercial product, process, or service by trade name, trademark, manufacturer, or otherwise, does not necessarily constitute or imply its endorsement, recommendation, or favoring by the United States Government or the University of California. The views and opinions of authors expressed herein do not necessarily state or reflect those of the United States Government or the University of California, and shall not be used for advertising or product endorsement purposes.

This is a preprint of a paper intended for publication in a journal or proceedings. Since changes may be made before publication, this preprint is made available with the understanding that it will not be cited or reproduced without the permission of the author.

# Nonlinear saturation of Stimulated Brillouin Scattering for long time scales

L. Divol, B. I. Cohen, E. A. Williams, A. B. Langdon, B. F. Lasinski.  
*Lawrence Livermore National Laboratory*  
*University of California P. O. Box 808, CA 94551, U.S.A.*

The nonlinear saturation of Stimulated Brillouin Scattering (SBS) in long Beryllium plasmas ( $500 \mu\text{m}$ ) and for long time (500 ps) is studied in detail through well-diagnosed 1D-hybrid PIC simulations (Bzohar[1]). Under conditions of interest, when the linear gain associated with the SBS growth is large, it is shown that following a first phase of large and bursty SBS reflectivity, SBS is suppressed by a self-induced spatial detuning due to inhomogeneous modifications of the (locally averaged) ion distribution function. This nonlinear evolution is generic over a wide range of laser intensities and plasma parameters.

PACS numbers: 52.25.Qt, 52.35.Fp, 52.40.Nk, 52.50.Jm

Understanding the nonlinear saturation of SBS in plasmas relevant to future fusion facilities such as the National Ignition Facility (NIF) is necessary to improve the energy coupling into the fusion capsule and to develop models that will predict SBS laser energy losses. The SBS instability results from the resonant coupling of an intense laser pulse with an ion-acoustic wave. The resulting driven ion-acoustic wave has been shown to saturate [2–4]. Various mechanisms have been suggested to explain ion-wave saturation, including frequency detuning induced by trapping [2, 4, 5], 2-ion-wave-decay [1, 6, 7], increased linear Landau damping due to kinetic ion heating [8, 9], nonlinear damping associated with wave-breaking and trapping [10, 11] or coupling with higher harmonics [12, 13]. In this letter, we describe the generic behavior of SBS observed in 1D-PIC simulations of long plasmas for long time, and suggest a new mechanism to explain the overall suppression of SBS at long time: a self-induced spatial detuning due to inhomogeneous modifications of the (locally averaged) ion distribution function.

We have done 1D-hybrid PIC (PIC ions and Boltzmann fluid electrons) simulations of a  $500 \mu\text{m}$  Be plasma with an electron temperature  $T_e = 430 \text{ eV}$ , ion temperature  $T_i = T_e/2$ , electron density  $n_e = 10^{20} \text{ cm}^{-3}$ , parameters representative of experiments done at TRIDENT [2]. The wavelength of the interaction beam is  $\lambda_0 = 0.53 \mu\text{m}$ , with intensity  $I_0$  in the range  $1.25 \times 10^{14} - 10^{15} \text{ W cm}^{-2}$ . This corresponds to  $n_e/n_c = 0.025$  and  $k_a \lambda_D = 0.4$ , where  $k_a = 2k_0$  is the wave vector of the SBS driven acoustic waves. Typically a spatial resolution of  $\Delta x = \lambda_D$  was used, with 100 particles per cell (higher resolution or particle number didn't show any significant differences). Fig. 1 shows the typical temporal evolution of the SBS reflectivity  $R_{\text{SBS}}$ . The laser intensity is ramped up to its peak value over 50 ps. One can see two successive phases: during the first 200 ps,  $R_{\text{SBS}}$  reaches large instantaneous values in a succession of short temporal peaks. Its time-averaged value, assuming a typical instrumental temporal resolution of 40 ps, also reaches increasingly large values with higher laser intensities but

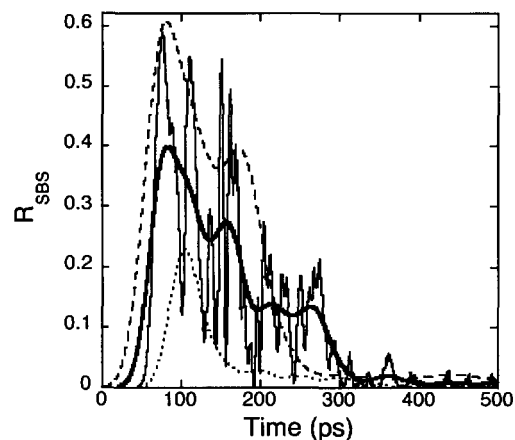


FIG. 1: Time evolution of the SBS reflectivity  $R_{\text{SBS}}$  for laser intensities  $I_0$  (in  $10^{15} \text{ W cm}^{-2}$  unit) equal to 0.125 (dotted), 0.25 (solid) and 1 (dashed). Curves are smoothed in time assuming a typical 40 ps instrumental resolution. The narrower solid curve is unsmoothed in time, with an intensity of 0.25, and exhibits fast temporal bursts.

shows that a much better temporal resolution is needed to resolve the bursts of reflectivity (this measurement will also require some spatial localization, using Thomson scattering for instance). Later,  $R_{\text{SBS}}$  is reduced to the percent level for all intensities, and remains at this low level until the end of the simulation. We now study in detail these two phases.

1) First, as the laser is ramped up, the amplitude of the acoustic wave grows from the fluctuation level. The linear amplitude gain exponent for SBS, assuming linear Landau damping, is 7.5 at the lowest intensity shown in Fig. 1, and the SBS instability quickly drives a large acoustic wave. One can estimate an effective damping  $\nu$  due to wave-particle interaction by comparing the rate of change of the local ion kinetic energy  $d_t K/K$  with the energy of the local acoustic wave, leading to  $\nu = \frac{d_t K/K}{2(\delta n/n)^2 Z T_e/T_i}$ . Fig. 2a shows that this damping is slightly larger than the theoretical linear ion Landau

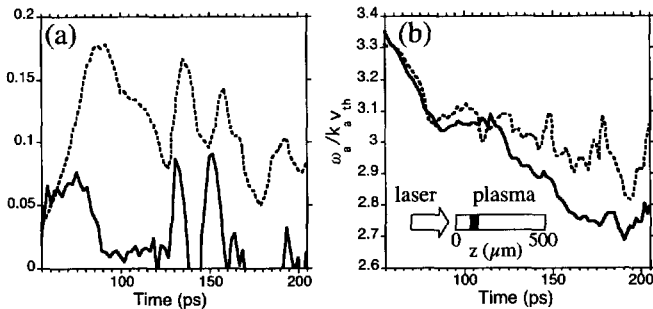


FIG. 2: a) shows the time evolution of the effective damping  $\nu/\omega_a$  (solid, defined in the text) and of the amplitude  $|\delta n/n|$  (dashed) of the SBS driven acoustic wave. b) shows the time evolution of the observed frequency of the SBS-driven acoustic wave (dashed), as well as the local frequency of the corresponding acoustic mode (solution of  $\epsilon(\omega_a, k = 2k_0) = 0$ , solid). The values plotted were calculated by averaging over  $25 \mu\text{m}$  around  $z = 100 \mu\text{m}$ , as shown in the figure. The laser intensity used was  $2.5 \times 10^{14} \text{ W cm}^{-2}$

damping ( $\nu_L/\omega_a = 0.05$ ) during the first rise of reflectivity (electron Landau damping would be 0.01 and is not included in these simulations). Nevertheless, the convective gain remains large and this energy loss is not able to stop the growth of the instability.

Indeed, once the reflectivity (and the driven acoustic wave amplitude) reaches its first peak value, energy transfer from the field into the particles decreases (Fig. 2a), as one can expect if enough ions with velocities in  $[v_\phi - \delta v]$  have been accelerated to  $[v_\phi + \delta v]$ , where  $\delta v \simeq v_\phi \sqrt{|\delta n/n|}$  is the trapping width and  $v_\phi \approx 3.17 v_{thi}$  the phase velocity of the SBS-driven acoustic wave, flattening the distribution function around  $v_\phi$ . At the same time, this modification of the distribution function reduces the local acoustic frequency from the linear value (Fig. 2b). This frequency shift detunes the three-wave-coupling process responsible for SBS, allowing energy transfer back into the pump wave [5], as shown in Fig. 3 resulting in a decrease of the amplitude of the driven acoustic wave. The solid curve in Fig. 2b shows the frequency corresponding to the linear response of the plasma when the locally-averaged ion distribution function has been modified, and is obtained by solving  $\epsilon(\omega_a, k_a) = 0$ . This does not include dynamic effects such as contributions from trapped particles. Hence, the detuning doesn't vanish with the acoustic wave. The dashed curve represents the frequency of the actual acoustic wave with wavenumber  $k_a$ , as determined by temporal windowed Fourier transform. This is the actual frequency of the SBS-driven acoustic wave that could be measured with Thomson scattering for instance. One can see that it follows the evolution of the local resonant frequency. The difference in frequency between the two curves is due to the fact that the backscattered light seen at a given position comes from parts of the plasma farther to the right,

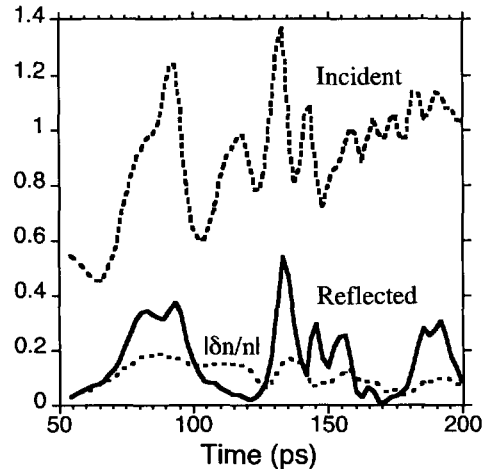


FIG. 3: Time evolution of the incoming light intensity (dashed), reflected light intensity (solid) and of the driven acoustic wave amplitude  $|\delta n/n|$  (dotted). Light intensities are normalized to the pump value at the entrance of the plasma. Values are averaged over the same sub-volume, with the same parameters as in Fig. 2.

and the resulting ponderomotive driver tends to be at a higher frequency than the downshifted local acoustic resonance (see below).

We will now show that some of the sudden decreases in the amplitude of the primary acoustic wave that follows the detuning of the instability are caused by decay of the primary wave into longer wavelength modes. Indeed, Fig. 4 shows the time evolution of the k-spectrum of acoustic waves. The steep drop in  $|\delta n/n|$  around  $t = 110 \text{ ps}$ , as well as the later drop at  $t = 180 \text{ ps}$ , coincides with the appearance of a broad spectrum of longer wavelength acoustic waves. The exact correlation in time between the energy loss from the (spectrally narrow) primary wave and the rise of the energy contained in the longer wavelength modes is evident on the line-outs plotted on the left part of Fig. 4. As was suggested by [1, 7], a frequency shift of the primary acoustic wave can help trigger the acoustic decay instability. Here, kinetic modifications of the ion distribution function produce such a negative shift, and the (Landau) damping has almost vanished, which reduces the decay threshold. Note that the effective damping  $\nu$  (Fig. 2a) fluctuates in time due to recurring wave-particle interaction when the acoustic wave reaches large amplitude, but is low when decay occurs. Using the dispersion relation from [1] to determine the growth rate of the decay instability, one finds that a 5% decrease in  $\omega_a$  is enough to transform the geometry of the decay process from a 2D problem to 1D, where the growth rate peaks for decay products along the primary wave vector and its peak value is increased. The wavelength of the decay products is very sensitive to the actual frequency mismatch, which is consistent with the

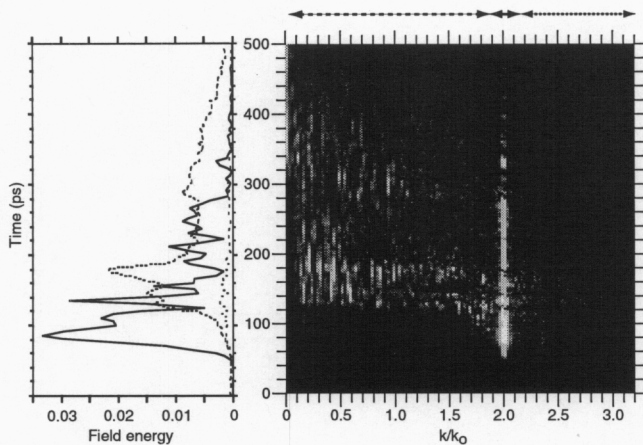


FIG. 4: Time evolution of the  $k$ -spectrum of acoustic waves (same sub-volume and parameters as in Fig. 2). Right, one can see the decay of the primary SBS-driven acoustic wave into longer wavelength modes. Left, lineouts show the energy transfer from the primary SBS-driven acoustic wave (solid) into the long wavelength modes (dashed). The dotted line shows the energy contained in the shorter wavelength modes.

observed broad spectrum in Fig. 4.

2) As seen in Fig. 1, time-averaging the oscillations of  $R_{\text{SBS}}$  shows an overall decrease of the reflectivity with time, until it stays below the percent level and the corresponding driven acoustic waves are down to  $|\delta n/n| < 0.01$ . This generic behavior is mostly independent of the laser intensity used to drive the SBS instability. This long time suppression of SBS can be explained by spatially inhomogeneous modifications of the ion distribution function. Driven by SBS, a large acoustic wave grows in the front of the plasma, while it remains smaller in the back of the plasma (following the usual convective growth picture). Wave-particle interaction (linear and nonlinear Landau damping, trapping and perhaps wave breaking) is thus stronger in the front, where the ion distribution function is more deeply modified than in the back, where it stays close to a Maxwellian. Consequently, the local acoustic frequency in the front of the plasma is smaller than in the back, and a spatial detuning of the instability occurs (Fig. 5). We would like to emphasize that the detuning is caused by a change in the quasi-linear response of the plasma arising from the modification of the locally-averaged (over a few acoustic wavelengths) distribution function. During the first phase described above, the front of the plasma sees a broadband spectrum of backscattered light coming from various depths (and thus corresponding to various resonant acoustic frequencies), which precludes the existence of any long-lasting BGK-like modes, as both the amplitude and frequency of the local acoustic wave vary quickly. This is probably different from what would happen in a simulation done using a fixed driver at a given frequency [14].

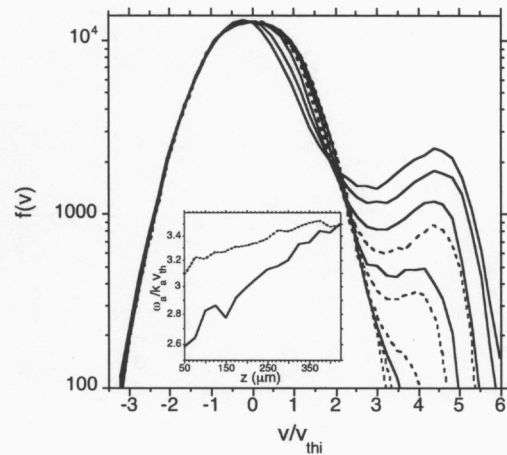


FIG. 5: Plot of the ion distribution function averaged over  $25\mu\text{m}$  every  $100\mu\text{m}$  in the plasma for  $I_0 = 0.125$  (dashed) and  $0.25 \times 10^{15} \text{W cm}^{-2}$  (solid), at  $t = 250 \text{ps}$ . This results in a spatial variation of the local resonant acoustic frequency corresponding to the SBS driven wave ( $k_a = 2k_0$ ), as shown in the insert. The steepest curve (solid) corresponds to the highest intensity.

To check this scenario, the simulation was stopped at  $t = 250 \text{ps}$ , when SBS has been suppressed, and restarted after having locally scrambled the ions: each particle was randomly moved in space (the displacements followed a gaussian distribution of width  $\lambda_0$ ). As a result, the locally averaged distribution function remained unchanged, but the coherent electrostatic fields (the driven acoustic waves and remaining decay products) were suppressed. SBS was found to stay at the same low level as before scrambling. It should be noted that the kinetic energy of the ions didn't increase in the rest of the simulation, ruling out an increased Landau damping due to the hot ion tail as a possible saturation mechanism. Indeed, the distribution function is relatively flat in the neighborhood of the phase velocity, suggesting that the Landau damping is reduced. Another attempt at restoring SBS was done by ramping up the laser intensity after  $t = 250 \text{ps}$  to four times its initial value. SBS then reappeared for a while, but vanished again after further modification of the distribution function.

These 1D simulations include no loss term (collisions [5, 8], transverse loss [14, 16]), and one can estimate the time needed for restoration of an homogeneous distribution function. Assuming for instance a  $60 \mu\text{m}$  wide focal spot [2], it takes  $1.2 \text{ns}$  for a thermal ion ( $v_{\text{thi}} = 0.05 \mu\text{m/ps}$ ) to go across the beam, and even assuming a Mach-2 transverse flow [2],  $v_\phi = 0.15 \mu\text{m/ps}$ , the characteristic loss time is  $200 \text{ps}$ . As noted before, the long-time detuning is due to modifications of the spatially averaged distribution function, so that ions leaving a hot spot inside the beam do not have to be in phase with

the local acoustic wave present in the neighbor hot spot to induce detuning: the transverse length that should be used to compute a loss rate due to advection is the width of the whole beam, not of a single speckle. This is different from what will happen in a so-called single speckle experiment, where the timescale of transverse loss is less than 10 ps.

Advection of hot ions (at  $v \simeq v_\phi$ ) along the laser propagation axis will also homogenize the distribution function, but this corresponds to a diffusion over only 37  $\mu\text{m}$  in 250 ps (compared to a plasma length of 500  $\mu\text{m}$ ).

Ion-ion collisions can be important in the cold plasma considered here and were neglected in the simulations. As the fast ions thermalize, energy (and momentum) is transferred from the tail into the bulk. This results in an inhomogeneous  $T_i$  throughout the plasma, leading to a gradient (that would be weaker than in the collisionless case) in the acoustic frequency, which increases compared to its initial value. This is consistent with the local increase in  $T_i$  observed in [2], which scaled with the local SBS-driven acoustic wave amplitude. The relaxation rate of a modified distribution function with a plateau of width  $v_{thi}$  around  $v_{phi}$  towards a Maxwellian is given by the parallel diffusion rate of fast ( $v \approx v_\phi$ ) ions in a background of thermal ions times  $(v_{phi}/v_{thi})^2$  which here gives  $\approx 5 \times 10^{10}\text{s}^{-1}$ . Non-local thermal effects could also result in an additional detuning, as the acoustic frequency depends on the local electronic temperature. Nevertheless, simulations done in a hotter plasma ( $T_e \simeq 1\text{keV}$ ), where collisions and non-local effects can be neglected, show that detuning by modification of the ion distribution function remains the main saturation process for SBS.

In summary, we have done a detailed study of the nonlinear evolution of SBS under laser/plasma conditions relevant to recent experiments done at the Trident facility [2]. A generic behavior of SBS is described, which consists in two successive phases. First the SBS reflectivity is large and fluctuates. These fast fluctuations were associated with nonlinear frequency shifts due to kinetic effects and sudden decays of the primary driven acoustic wave into longer wavelength modes. The large acoustic waves driven during this first phase modify in an inhomogeneous way the ion distribution function, which spatially detunes the instability, as the acoustic frequency is no longer constant throughout the plasma. As the time needed to restore an homogeneous distribution function (through advection, transverse loss or collisions) is very long, SBS remains low for the rest of the simulation. This picture of the nonlinear saturation of SBS remains true over a broad range of intensities, and is consistent with earlier 2D simulations [1, 7] which showed a large SBS reflectivity early in time followed by a low reflectivity later in the simulation. It could also explain SBS measurements from CH gasbags [15] that usually show a large

SBS only during the first part of the interaction. This saturation mechanism for long-time SBS should hold as long as hot ions advect over a short length compared to the plasma length (i.e.  $\sqrt{ZT_e/MT_{\text{pulse}}} \ll L_{\text{plasma}}$ ), which is usually fulfilled for ignition-relevant plasmas, and kinetic effects are important (i.e.  $ZT_e/T_i \leq 20$ ), so that a relatively small modification of the ion distribution function around the sound speed results in a large frequency shift for acoustic waves. We note that a reduced model [2, 16] of this saturation mechanism has to follow the evolution of the distribution function and be non-local in time, as late in the simulations a large frequency shift remains while the driven acoustic waves have almost vanished. As a result, the steady-state model we used in [2] can not be immediately generalized to a time-dependent model but remains useful for a qualitative estimate of trapping-induced detuning of SBS.

The first author would like to thank S. H. Glenzer and D. H. Froula for fruitful discussions on experimental evidences of nonlinear saturation of SBS. This work was performed under the auspices of the U.S. Department of Energy by the Lawrence Livermore National Laboratory under Contract No. W-7405-ENG-48.

- 
- [1] B. I. Cohen *et al.*, Phys. Plasmas **4**, 956 (1997).
  - [2] D. H. Froula, L. Divol and S. H. Glenzer, Phys. Rev. Lett. **105**003 (2002).
  - [3] S. H. Glenzer *et al.*, Phys. Rev. Lett. **86**, 2565 (2001).
  - [4] C. E. Clayton, C. Joshi and F. F. Chen, Phys. Rev. Lett. **51**, 1656 (1983); H. Ikezi, K. Schwarzenegger and A. L. Simons, Phys. Fluids. **21**, 239 (1979).
  - [5] A. A. Andreev and V. T. Tikhonchuk, Sov. Phys. JETP **68**, 1135 (1989); R. E. Giacone and H. X. Vu, Phys. Plasmas **5**, 1455 (1998); H. X. Vu, D. F. DuBois and B. Bezzerides, Phys. Rev. Lett. **86**, 4306 (2001).
  - [6] W. L. Kruer, in *From fusion to light surfing*, edited by T. Katsouleas (Addison-Wesley, Redwood City, Ca., 1991), p. 167.
  - [7] C. Riconda *et al.*, Physica Scripta **84**, 217 (2000).
  - [8] P. W. Rambo, S. C. Wilks and W. L. Kruer, Phys. Rev. Lett. **79**, 83 (1997).
  - [9] C. J. Pawley, H. E. Huey and N. C. Luhmann, Jr., Phys. Rev. Lett. **49**, 877 (1982).
  - [10] W. L. Kruer, Phys. Fluids **23**, 1273 (1980).
  - [11] M. J. Herbst, C. E. Clayton and F. F. Chen, Phys. Rev. Lett. **43**, 1591 (1979); J. Handke, S. A. H. Rizvi and B. Kronast, Phys. Rev. Lett. **51**, 1660 (1983); J. E. Bernard and J. Meyer, Phys. Rev. Lett. **55**, 79 (1985).
  - [12] W. Rozmus *et al.*, Phys. Fluids **B4**, 576 (1992).
  - [13] J. A. Heikkinen, S. J. Karttunen and R. R. E. Salomaa, Phys. Fluids **27**, 707 (1983).
  - [14] H. A. Rose and D. A. Russell, Phys. Plasmas **8**, 2439 (2001).
  - [15] J. D. Moody *et al.*, Phys. Rev. Lett. **86**, 2810 (2001).
  - [16] H. X. Vu, D. F. DuBois and B. Bezzerides, Phys. Plasmas **9**, 1745 (2002).